



Mechanical Properties, Resistance to Fire and Durability for Sulfate Ions of Alkali activated Cement made from Blast Furnace Slag-Fine Metakaolin



CrossMark

O. Fadel¹, E.E. Hekal², F.S. Hashem^{2*}, F.A. Selim²

¹ Laboratories Department, The Arab Contractors (Osman Ahmed Osman & Co.), Cairo, Egypt.

² Chemistry Department, Faculty of Science, Ain Shams University, Cairo, Egypt.

Abstract

The characterization of alkali activated cement prepared by blending blast furnace slag (BFS) and fine metakaolin (FMK) is studied. MK of particle size 45 μm and blain area 6530 cm²/kg is used by 20, 40, 60 and 80% replacement of BFS in the production of alkali activated cement. The utilized alkaline activator is mixture of NaOH and Na₂SiO₃ with various molar ratios. The prepared specimens are cured under humidity conditions up to 90 days. All specimens are characterized regarding setting times, compressive strength and water absorption. The formed hydrates are studied using XRD analysis, FTIR spectroscopy and SEM technique. The durability of the prepared geopolymer is determined via studying the fire resistance at 300°, 600° and 800 °C and sulfate ions attack after time intervals extended up to 1 year. The results indicate that the specimens made from 60% BFS and 40% FMK and activated by (1:1) NaOH and Na₂SiO₃ were revealed the best overall behaviour.

Key words: Geopolymer; Slag; Metakaolin; Thermal resistance; Sulphate resistance

1. Introduction

Portland cement is the most common material used in civil engineering fields. However, Portland cement production causes emission of huge amount of both carbon dioxide (CO₂) and toxic fumes into the surrounding atmosphere. Approximately, about 0.94 tonnes of CO₂ are emitted into the atmosphere in manufacture of 1 tonnes of cement [1]. Besides, manufacturing of Portland cement requires a high demand of energy, mostly consumed during clinker manufacturing process [2].

Geopolymer cement (GPC) or alkali-activated cement is considered the best alternative material for Portland cement [3]. In contrary to OPC, geopolymer cement, does not depend on firing of limestone, which is the major source of CO₂ emission in the production of OPC [4, 5]. Geopolymer cement is made by mixing

of aluminosilicate precursors with highly concentrated alkali activated solution through geopolymerization process. It is made of chains with three dimensional replicate structures of (Si –O –Al –O –)_n and (Si –O –Al –Si –O –)_n units [6]. The transformation of a solid aluminosilicate precursor into gelatinous geopolymer matrix of high compact structure occurred in three main steps. During the first one, the dissolution of the amorphous aluminosilicate source by the action of the alkali solution is happened that it creates a supersaturated solution of SiO₂ and Al₂O₃ species. These species are connected together leading to the creating of gelatinous networks while water is released gradually. In the final step, the gel network increased that allows the formation of three dimensional geopolymer matrices [7, 8].

According to the previous research data, geopolymer binder offers high mechanical properties,

*Corresponding author e-mail: f_s_hashem@ymail.com.

Receive Date: 22 April 2020, Revise Date: 11 May 2020, Accept Date: 19 May 2020

DOI: 10.21608/EJCHEM.2020.28427.2612

©2020 National Information and Documentation Center (NIDOC)

good firing (up to 1000°C) and acid resistivity [9, 10]. However, the mechanical properties and performance of geopolymer cement are highly dependent on many factors including, (i) the aluminosilicate precursor, (ii) the alkaline activator solution and its dosage as well as the (iii) curing conditions [11-15].

Blast furnace slag (BFS) is a by-product produced from iron blast furnace after rapid quenching in water or air. It is composed mainly from mixture of CaO, SiO₂, MgO and Al₂O₃. BFS based GPC offers high resistance to different acids and salt solutions with low thermal conductivity [15-17]. Metakaolin (MK) is a pozzolanic material that is generated by firing of kaolinitic clay at temperature between 650 °C and 800 °C. MK is one of the main common aluminosilicate precursors materials which used in the manufacture of geopolymers [18-20]. The composition, structure and properties of the reaction products obtained in the alkali activation of metakaolin are directly impacted by the specific surface and composition of the initial kaolin.

The objective of this investigation is to evaluate the geopolymer cement based on BFS and BFS/FMK prepared by various Na₂O molar ratios. In addition, the resistance towards fire; up to 800°C, and attack by SO₄²⁻ ions; up to 1 year, of the prepared geopolymer is determined.

2. Experimental Program

2.1. Raw Materials and Chemicals

The utilized starting materials for the geopolymer cement composites synthesis are:

1- Fine Metakaolin (FMK) of particle size 45 μ was supplied from Asfour Company for Mining and Refractories in Helwan province, Egypt. It's a fine by-product, having Blaine specific surface area of 6530 cm²/kg.

2- Blast-furnace slag (BFS) is sourced from iron and steel factory located in Helwan province, Egypt having Blaine specific surface area of 2883 cm²/kg.

3- A commercial sodium silicate solution (water glass) was supplied from the market with the module ($M = n_{SiO_2} / n_{Na_2O} = 3.0$). Sodium hydroxide pellets 98% with 10M concentration and Magnesium sulfate powder were provided from Alfa aromatic company. The chemical compositions of starting materials are

given in Table (1). The XRD of BFS and MK materials are given in Figure (1).

Table (1): The chemical compositions of starting materials, wt %

Oxide %	BFS	FMK
SiO ₂	38.9	52.83
Al ₂ O ₃	10.66	38.46
Fe ₂ O ₃	1.20	0.91
CaO	38.51	7.32
MgO	4.39	0.13
SO ₃	1.96	0.01
K ₂ O	0.49	0.06
Na ₂ O	0.91	0.03
Cl	0.04	0.02
L.O.I	2.94	0.23

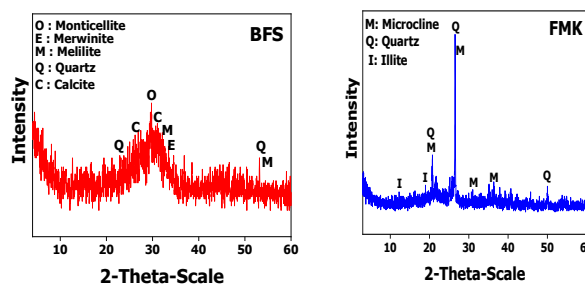


Figure (1): XRD pattern for BFS and Fine Metakaolin

2.2. Mixes design

Various geopolymer mixes are prepared using BFS and FMK. Table (2) illustrates the composition of different mixes and their notation. The alkaline activator used is a mix of sodium silicate solution (water glass) and NaOH (10M). Na₂SiO₃/NaOH ratios used were as follow: 2.5, 2, 1.5, 1, 0.7, 0.5 and 0.4.

2.3. Geopolymer preparation and curing

Each paste was prepared by mixing each dry mix with constant liquid activator/solid ratio=2:1. After complete mixing of each dry mix, the resulted pastes were moulded into cubic specimens by using one - inch cube moulds. The moulds containing the pastes were cured in humidity air for the first 24 h then the hardened pastes were removed from the moulds and cured at ~ 100 % RH atmosphere up to 90 days.

Table (2): The designed geopolymer mixes.

Mixes	Mix proportion (wt, %)		Activators %	
	BFS	FMK	Na ₂ SiO ₃	Na OH
M1	100	0	2.5	1
M2	100	0	2	1
M3	100	0	1.5	1
M4	100	0	1	1
M5	100	0	1	1.5
M6	100	0	1	2
M7	100	0	1	2.5
M8	80	20	1	1
M9	60	40	1	1
M10	40	60	1	1
M11	20	80	1	1
M12	0	100	1	1

2.4. Test procedure

2.4.1. Setting times

Initial and final setting times of fresh BFS/FMK based geopolymer were tested using a Vicat apparatus (RV-300B, China).

2.4.2. Compressive strength and Water absorption

Three samples of each mix are used to determine water absorption (%) and compressive strength. The compressive strength was carried out using a Ton Induric machine (West Germany) for maximum load of 60 tons.

2.4.3. Durability tests

To evaluate the durability of the GPC specimens towards deteriorations of firing and attack by sulfate ions are studied. Attack by sulfate ions is studied as follow: after 28 days of curing, the cubic specimens are immersed into 5% MgSO₄ solution for 1 year. MgSO₄ solution is renewed changed regularly. Compressive strength and percentage of mass change is determined for each specimen after 1, 3, 9 and 12 months. Firing resistance is tested by heating 28 -days hardened GPC specimens at 300°, 600° and 800°C for three h.

Phase composition, and microstructures of GPC are tested by XRD, FTIR and scanning electron microscopy techniques. XRD was performed using cobalt target ($\lambda = 0.17889$ nm), and filter made of

nickel under 40 kV and 40 mA. SEM examinations were done using SEM Model Quanta 250 FEG (Field Emission Gun). FTIR spectra was used to analyze GPC specimens using a Fourier transform infrared spectrometer (BIO-RAD FTS-40).

3. Results and discussion

3.1. Characterization of Precursors Materials

XRD of BFS and FMK are illustrated in Figure 1. BFS is mainly amorphous material which is composed mainly of mullite (Al₂(SiO₄)O), calcite (CaO) and minor amounts of quartz (SiO₂). FMK is composed mainly from crystals of quartz (SiO₂) and illite.

3.2. Setting Times

Initial and final setting times of geopolymer mixes made from 100% BFS and activated by solutions of various (Na₂SiO₃/NaOH) ratios; M1, M2, M3, M4, M5, M6 and M7 mixes, are illustrate in Figure (2). Mix made from 100% BFS and activated (Na₂SiO₃/NaOH) =2.5; M1 mix, shows the shortest initial and final setting times of all prepared geopolymer mixes. Besides, the setting times increased by decreasing (Na₂SiO₃/NaOH) ratio from 2.5 to 0.4. M7 mix activated by blends made with (Na₂SiO₃/NaOH) ratio of 0.4 exhibits the longest initial and final setting times compared to those made with other ratios. Such results can be attributed to the reduction in the amount of soluble Si present in the mix by decreasing (Na₂SiO₃/NaOH) ratio, which it results in slow down the polymerization process [21]. In addition; when the sodium hydroxide solution is added into sodium silicate solution, it may lower the viscosity of the paste; therefore, the geopolymer system needs more time for initial setting [22].

Setting times of geopolymer mixes made from BFS/FMK and activated by (Na₂SiO₃/NaOH) ratio =1, M4, M8, M9, M10, M11 and M12 mixes, are illustrate in Figure (3). Replacing BFS with FMK (0, 20, 40, 60, 80 and 100% by mass of BFS) causes a notable delay in the setting process. Also, setting times enlarged as the contents of FMK increases in the geopolymer paste. This could be related to the replacing of BFS (calcium-rich material) by FMK (less calcium contents materials) causes reducing in the forming calcium silicate hydrate (CSH) gel in addition to the sodium aluminum silicate hydrate (NASH) gel (geopolymer gel) [23]. BFS decreases the alkaline liquid consistency and accelerates the hardening of geopolymer paste [24].

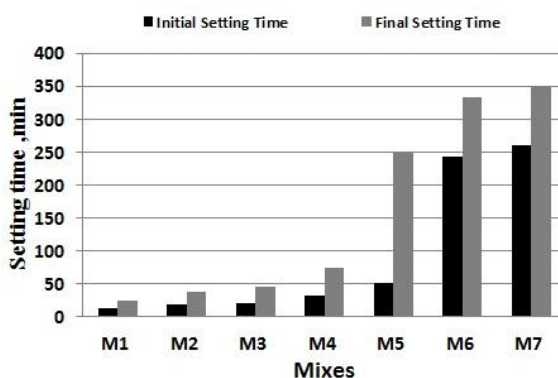


Figure (2): Setting time of BFS geopolymer

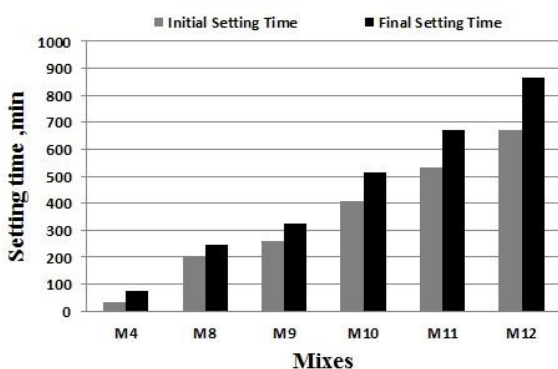


Figure (3): Setting times of BFS/FMK based geopolymer

3.4. Compressive Strength

The results of compressive strength of M1, M2, M3, M4, M5, M6 and M7 mixes are illustrated in Figure (4). All geopolymer mixes show that compressive strength increases gradually with increasing curing ages up to 90 days. This can be related to the higher reactivity of BFS, which in the presence of alkaline activator ($\text{Na}_2\text{SiO}_3/\text{NaOH}$ mix), the bonds between $\text{Ca}=\text{O}$; $\text{Si}=\text{O}$ and $\text{Al}=\text{O}$ are broken. This dissolves and promotes the formation of species as Ca^{2+} ; $[\text{H}_2\text{SiO}_4]^{2-}$, $[\text{H}_3\text{SiO}_4]^-$ and $[\text{Al}(\text{OH})_4]^-$ which precipitate when their concentrations reach super saturation forming CSH and CASH gels. The precipitation of CASH gels leads to initiate the polymerization reactions leading to rapid hardening [25]. Besides, the calcium ions exist in BFS enter in the $\text{Si}=\text{O}=\text{Al}$ gel structure, which neutralizes the charge of the aluminum atoms (Al^{3+}) and allows space for CASH system in addition to NASH gel. This leads to the formation of a more-denser structure [26].

Mix 4; activated by mixture of ($\text{Na}_2\text{SiO}_3/\text{NaOH}$) ratio = 1.0 exhibits the highest compressive strength than those with another ratio at all curing ages. This reveals the impact of the concentration of the alkaline activator constituents. The compressive strength is expected to decrease as more silicate is added into the system. This is because excess sodium silicate lower water evaporation and structure formation. Such conclusions agree with the results of [27, 28] that the high activator concentration has negative effect on the strength.

The results of compressive strength values of BFS/FMK geopolymer mixes; M4, M8, M9, M10, M11 and M12 mixes at various curing times are graphically represented in Figure (5). Obviously; the compressive strength of these mixes increases with increasing the curing time. When 20% of BFS is substituted by FMK, mix M8, deterioration in compressive strength is obtained. The compressive strength of mix M9 exhibits approximately five fold high as compared with 100% FMK-based sample (M12). This is attributed to the reaction of Ca^{+2} ions supplied by BFS with silicates ions leads to form additional strength-giving gel [29]. From we can conclude that Ca^{+2} ion plays the key role in geopolymer formation. In fact, the high CaO content accelerates the geopolymerization and development of semi-crystalline CASH hydrate gel produced from reaction between calcium silicate hydrate (CSH) and aluminosilicate group [30].

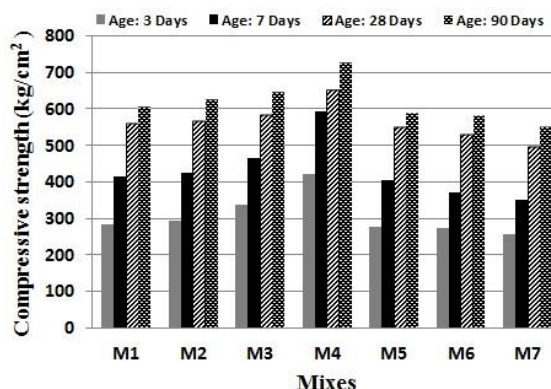


Figure (4): Compressive strength of BFS geopolymer

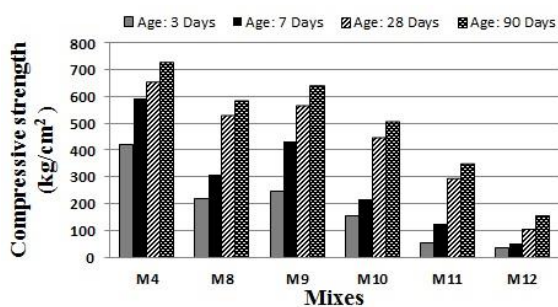


Figure (5): Compressive strength of BFS/FMK based geopolymer

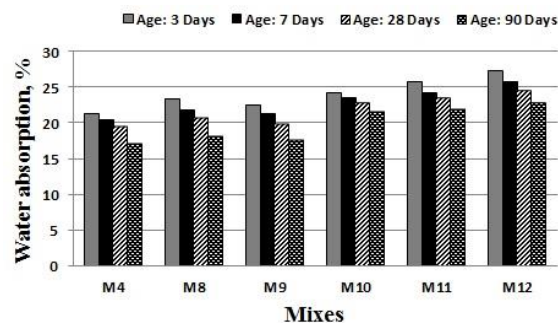


Figure (7): The Water absorption of BFS/FMK based geopolymer

3.4. Water absorption

Water absorption is considered an indicator for the degree of geopolymeric reaction. Water absorption (%) of M1, M2, M3, M4, M5, M6 and M7 mixes are illustrated in Figure (6). It is clear that the water absorption values of all mixes decrease with curing time. It related to the progress of the polymerization reactions and changes the matrix to more compact structure with lower porosity. Besides, the water absorption (%) values for M4 mix are the lowest indicating the least porosities are formed in this mix.

Water absorption (%) of geopolymer mixes made by replacement of BFS by FMK at various curing times are represented in Figure (7). It was clear that the water absorption values of all mixes decrease with curing time. With increasing FMK content, the water absorption is increased. Presences of FMK in geopolymer matrix, activation (Si+Al) occurred beside (Si+Ca) leading to the formation of CASH with geopolymer network. However, increasing FMK contents increases the formation of CASH gel and decrease the CSH gel inside the GPC matrix.

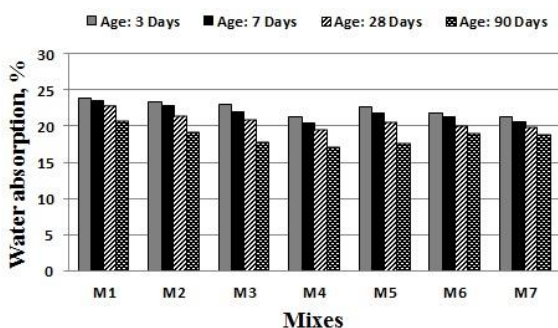


Figure (6): Water absorption of BFS geopolymer

3.5. Resistance to sulfate attack

Among the studied mixes, M2, M3, M4, M8 and M9 mixes are selected to test their resistance against exposure to 5% magnesium sulfate solution. The Compressive strength of M2, M3, M4, M8 and M9 mixes after immersing in 5% $MgSO_4$ solution up to 12 months are represented in Figure (8). Also, the percentage of mass change values of this mixes are represented in Figure (9).

According to Figure 8, all mixes show a continues decrease in compressive strength by increasing the curing time in magnesium sulfate solution. Besides, the mass of these mixes increasing with the curing times. This may be attributed to the attacks of SO_4^{2-} ions to the geopolymer matrix through series of deteriorations reactions leading to the formation of new phases like gypsum and ettringite [31]. Presences of such phases inside the hardened geopolymer matrix; which they are characterized by their large volumes, induces an internal stress. Such stress leads to formation of micro cracks and migration of alkalis from geopolymers into the solution within pores [32]. Partial replacement of BFS by 20% and 40% FMK, mixes M8 and M9 respectively, leads to decrease in the loss in compressive strength due to immersion in sulfate solution, Figure 9. This can be related to the partial filling of the pores by FMK. The filling effect of FMK decreases the permeability and entrance of SO_4^{2-} ions inside the core structure of geopolymers.

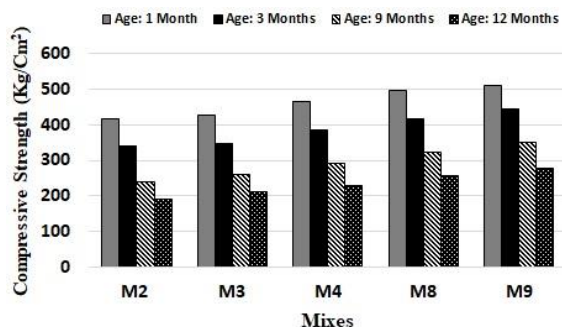


Figure (8): Compressive strength of M2, M3, M4, M8 and M9 mixes after immersing in $MgSO_4$

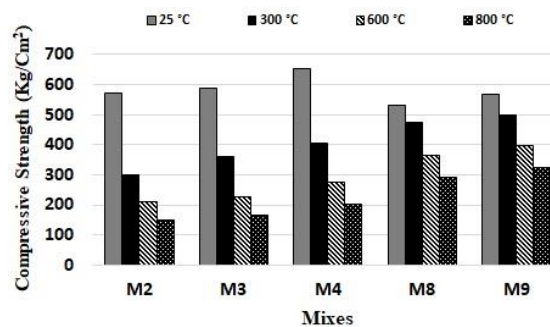


Figure (10): Compressive strength of M2, M3, M4, M8 and M9 mixes after firing at different temperature

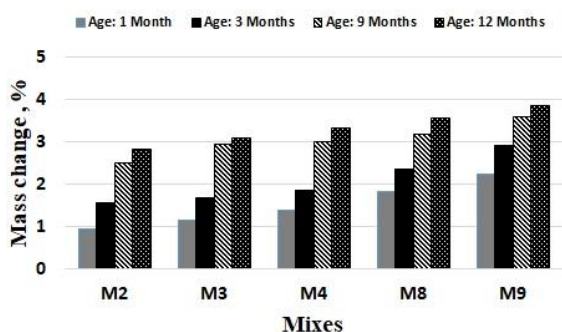


Figure (9): Mass change of M2, M3, M4, M8 and M9 mixes after immersing in $MgSO_4$

3.6 Fire Resistance:

GPC specimens made from M2, M3, M4, M8 and M9 mixes after curing for 28 days in 100% RH are fired at 300, 600 and 800 °C for 3hrs. Heating all GPC specimens resulted in a continuous loss in compressive strength; Figure 10. The decrease in compressive strength can be attributed to the dehydration and decalcination of GPC hydrates that leads to cracks formation and pores broadening [33]. GPC made from BFS/FMK specimens, mix M8 and M9, show reduced loss in the compressive strength upon firing at 800°C compared to those made from 100% BFS. About 55 and 41% of the strength still retained by M8 and M9 specimens respectively while 26, 28 and 30% are recorded for M2, M3 and M4 respectively. This indicates the high resistance for firing exhibit by GPC made from BFS/FMK.

3.7. Phase composition

XRD diffraction patterns of GPC specimens made from Mixes M4, M8 and M9 after 3 and 28 days of curing in 100% RH, are shown in Figure 11. The diffraction patterns of M4 specimens after 3 days of curing displays characteristics peaks due to CSH gel [34, 35] and calcite. In M8 and M9 specimens, new crystalline phases including thomsonite (CASH) gel and Garronite (NCASH) are formed due to slag alkali-activated reactions. Garronite (NCASH) has also previously been detected in alkali-activated slag/metakaolin geopolymers produced from strong activator concentration [36]. Peaks due to unreacted quartz are also identified in these samples.

After 28 days of curing, the intensities of the hydrated phases increase while as the intensity of quartz decreased indicating the progress of the polymerization reactions.

XRD of mixes M4 and M9 after 1 and 4 months of immersing in 5% $MgSO_4$ are shown in Figure 12. Peaks characterized to CSH gel are appeared in M4 specimen after 1 month while they nearly disappeared after 9 months of curing in $MgSO_4$ solution. This reveals the deterioration occurred in this mix made from 100% slag. However, for GPC made from BFS/FMK, mix M9, NCASH peaks are still appeared in XRD patterns up to 9 months. This confirms the compressive strength results that GPC made from BFS/FMK shows resistance to sulfate attack compared to GFC made from 100% slag.

XRD of mixes M4 and M9 after firing at 300° and 800°C for three h is shown in Figure 13. XRD patterns of the M4 mix after firing at 800°C show peaks that corresponding to Gehlenite, NASH. While the observed resistance for firing by M9 specimens at

800°C is confirmed by the increased intensities for NASH peaks.

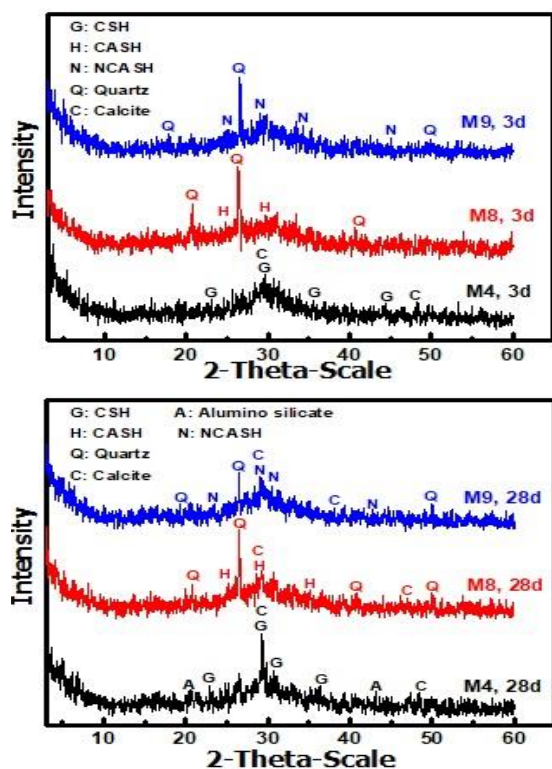


Figure (11): XRD patterns for hardened paste of mixes M4, M8 and M9 after 3 and 28 days of curing in 100% RH

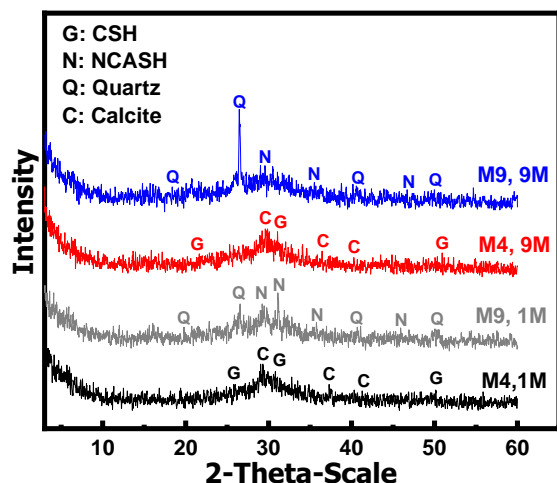


Figure (12): XRD patterns for hardened pastes of mixes M4 and M9 after 1 month and 9 months of curing in 5% MgSO₄

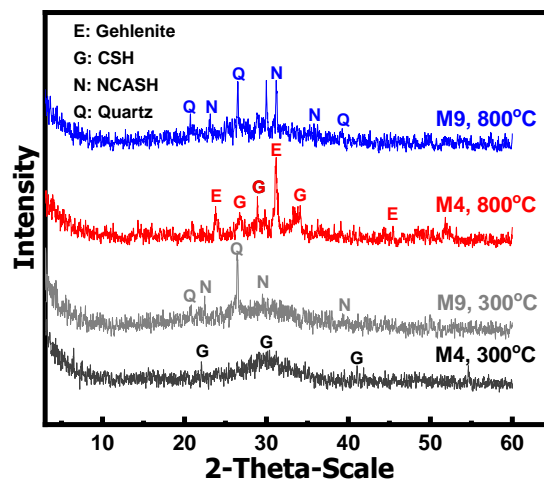


Figure (13): XRD patterns for hardened paste of mixes M4 and M9 after firing at 300 and 800°C

3.8. Microstructure

SEM of M4 and M8 specimens after curing for 3 and 28 days are shown in Figure 14a-d. After 3 days, SEM micrographs of M4 mix, Figure 14-a, shows slag particles that are covered by geopolymer hydrates mainly CSH gel and CASH indicating the start the geopolymer reactions. CASH acts as nucleation centers for geopolymerization [37]. After 28 days a dense and compact of gel like structure consists of ill crystalline and gelatinous CSH gel and CASH that are appeared in SEM micrographs.

For M8 mix, loose structure and FMK particles are appeared in SEM micrograph after 3 days of curing, Figure 14-c. According to Z. Li, et al, GPC made from metakaolin suffer from chemical shrinkage due to the continuous dissolution of the precursor to form monomers or small oligomers. However, after 28 days, SEM micrograph of this mix shows a chain composed mainly of geopolymer products that are intermix of CASH and NASH. Formation of these chains is confirmed the continues of polymerization process in which the chains are connected the FMK particles. Also the According to previous works, the presence of aluminum and silicon ions in FMK geopolymer supports the development of cementitious gels like Al-rich gel and Si-rich gel and decreasing the formation of CSH gel [38, 39].

After firing at 300 °C for three hrs, SEM micrograph of M4 mix shows loose structure of observed cracks and pores. However, After firing at 800°C, deep and large cracks are appeared that indicating the deterioration effects occurred, Figure 15 a,b. M8 mix after firing at 300° and 800°C, still keep a compact

structure of rug-like shape of geopolymer products with limited pores are appeared after firing at 800°C. This is explained the resistance of this mix to effect of heating, Figure 15-c,d.

SEM micrographs of M4 mix after immersion in 5% MgSO₄ solution for 1 and 9 months, Figure 16a-d., show slag particles that are partially covered with fine needle-like crystals of ettringite which they have a negative effect on compactness. Limited crystals of ettringite in M8 mix are observed after curing for 1 and 9 months in 5% MgSO₄ solution.

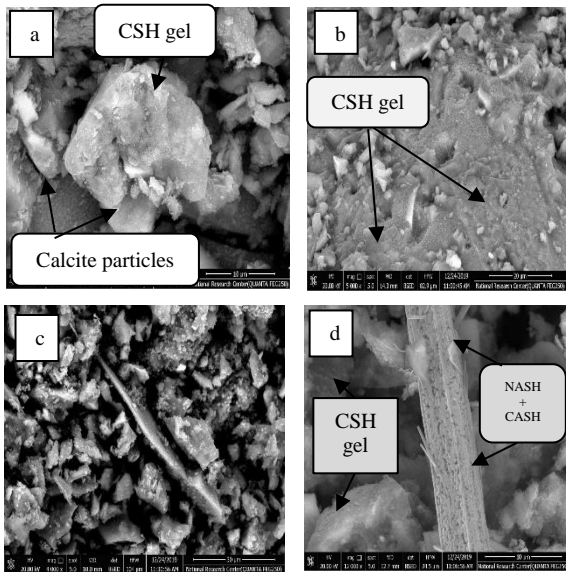


Figure (14): SEM micrographs of a) M4 after 3 days b) M4 after 28 days c) M8 after 3 days d) M8 after 28 days of curing

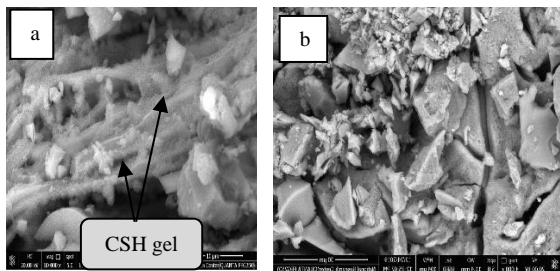


Figure (15): SEM micrographs of geopolymer after firing a) M4 mix 300 °C b) M4 at 800 °C

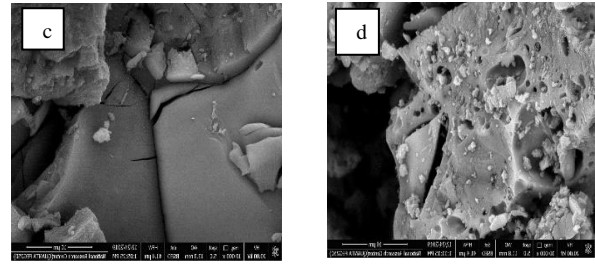


Figure (15): SEM micrographs of geopolymer after firing c) M8 mix at 300 °C d) M8 mix at 800 °C

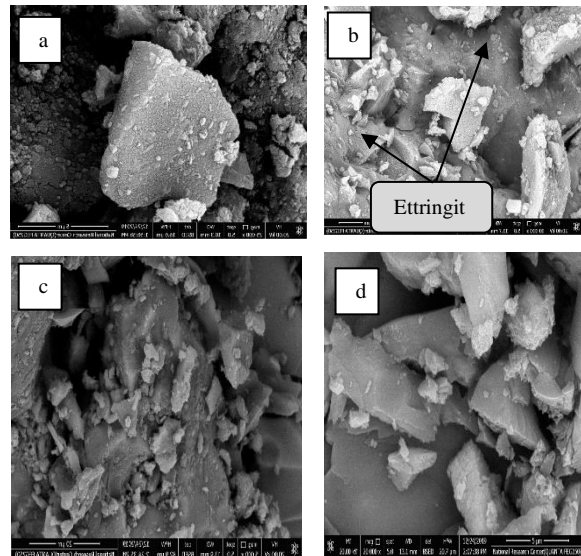


Figure (16): SEM micrographs of geopolymer after immersion in MgSO₄ solution a) M4 mix for 1-month b) M4 mix for months c) M8 mix for 1-month d) M8 mix for 9 months.

3.9. FTIR spectroscopy

FTIR spectra of geopolymer samples prepared from M4, M8 and M9 mixes after 28 days of curing are shown in Figure 17a. FTIR spectra of all GPC specimens show abroad band appearing in the range of 3440-3450 cm⁻¹ which represent the stretching vibration of O-H and H-O-H bonds due to water molecules adsorbed or embedded in pores during polymerization [40]. The band at 1450 cm⁻¹ indicated the stretching vibration of O-C-O was detected for all tested GPC pastes which is attributed to the carbonation reaction. The band between 980 and 1027 cm⁻¹ is attributed to asymmetric stretching vibration of Si-O-Si and Al-O-Si band of CSH and CASH gel. Also was found stretching vibration of Si-O-Si at

660 cm^{-1} and bending vibrations of Si-O-Si and O-Si-O located at 450 cm^{-1} .

IR spectra M8 and M9 specimens after show a notable increase in the intensity at 1450 and 1027 cm^{-1} of Si-O-Si and Al-O-Si. This is indicated that the formation of MK geopolymer in the presence of high rich calcium provided materials supports the simultaneous development of cementitious gels CASH and NASH type gels. According to [41] Ca^{2+} ions are supposed to be coupled with the Si-O-Al framework of geopolymeric gel, participating in balancing of negative charge species in tetrahedral Al (III) and replacing the alkali cations.

The durability behavior due to attack by sulfate ions or firing of M4 and M9 mixes are clearly shown in their FTIR spectra, Figure 17 b,c. After immersion in sulfate ions solution for 1 and 9 months, M9 mix shows an increasing in intensity of the peaks at 1027 and 450 cm^{-1} due to Al-O-Si and Si-O-Si bonds in contrary to M4 mix. Also, this noticed for the same mix after firing at 300° and 800°C. Such note indicates the substitution of BFS by 40% FMK increases the resistivity of the formed GPC toward attack by fire or sulfate ions.

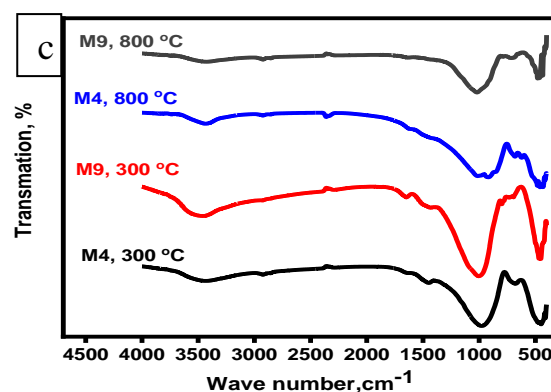
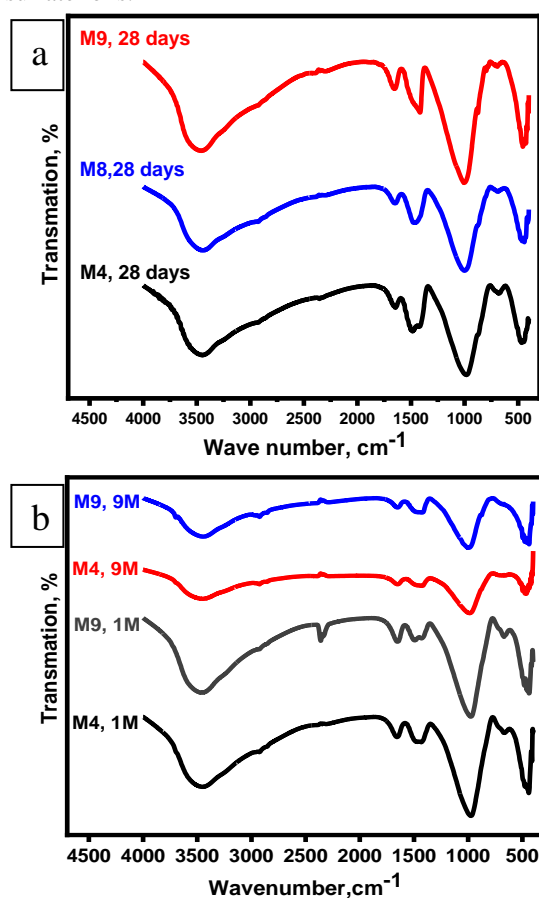


Figure (17): FTIR-spectra of M4, M8 and M9 mixes after a) 28 days of curing b) immersion in Sulfate and c) firing

Conclusion

The following conclusions can be drawn from the experimental results:

- 1-Setting times of BFS/FMK based geopolymer cement increases by decreasing ($\text{Na}_2\text{SiO}_3/\text{NaOH}$) ratio from 2.5 to 0.4 and increasing the contents of FMK.
- 2-GPC made from 60% BFS and 40% FMK and activated by mixture of ($\text{Na}_2\text{SiO}_3/\text{NaOH}$) ratio = 1.0 exhibits the best mechanical properties, least water absorption among the studied mixes.
- 3-All GPC mixes made from BFS/FMK blends show high durability towards attack by SO_4^{2-} ions up to 9 months and firing up to 800°C.
- 4-According to XRD, FTIR studies, the main phases in GPC made from 100% BFS is CSH gel and CASH. CASH acts as nucleation centers for geopolymerization.
- 5- In GPC made from BFS/FMK, a rug-like of geopolymer products; mainly NCASH and CASH gel, are appeared in SEM micrographs.
- 6-The formation of such geopolymerization products explains the high resistivity of the formed GPC toward attack by fire or sulfate ions.

Conflicts of interest

“There are no conflicts to declare”.

3. References

- [1] W. Shen, Z. Cai, Z. Liu, Humble talk about low carbon dioxide emission technique for cement-concrete industry, *Cement Guide for New Epoch* 14(4) (2008) 1-6.
- [2] M. Schneider, M. Romer, M. Tschudin, H. Bolio, Sustainable cement production—present and future, *Cem. Concr. Res.* 41(7) (2011) 642-650.
- [3] M.L. Berndt, Properties of sustainable concrete containing fly ash, slag and recycled concrete aggregate, *Construction and building materials* 23(7) (2009) 2606-2613.
- [4] B.V. Rangan, Design and manufacture of flyash-based geopolymer concrete, *Concrete in Australia* 34(2) (2008) 37-43.
- [5] G. Habert, N. Roussel, Study of two concrete mix-design strategies to reach carbon mitigation objectives, *Cement and Concrete Composites* 31(6) (2009) 397-402.
- [6] H. El-Didamony, A.A. Amer, S. El-Hoseny, Recycling of low-grade aluminosilicate refractory brick waste product in blended cement, *Journal of Thermal Analysis and Calorimetry* 125(1) (2016) 23-33.
- [7] J.L. Provis, S.A. Bernal, Geopolymers and related alkali-activated materials, *Annual Review of Materials Research* 44 (2014) 299-327.
- [8] A.P. Mora, M. Coulibali, W. Zhang, N. Tessier-Doyen, E. Thune, M. Huger, Monitoring the Structural Evolution during Geopolymer Formation by ^{27}Al NMR, *UNITECR* 2019, 2019.
- [9] M.-c. Chi, J.-j. Chang, R. Huang, Strength and drying shrinkage of alkali-activated slag paste and mortar, *Advances in Civil Engineering* 2012 (2012).
- [10] J. Davidovits, Application of Ca-based geopolymer with blast furnace slag, a review, 2nd International Slag Valorisation Symposium, 2011, pp. 33-49.
- [11] M. Juenger, F. Winnefeld, J.L. Provis, J. Ideker, Advances in alternative cementitious binders, *Cem. Concr. Res.* 41(12) (2011) 1232-1243.
- [12] A. Hajimohammadi, J.S. van Deventer, Characterisation of one-part geopolymer binders made from fly ash, *Waste and biomass valorization* 8(1) (2017) 225-233.
- [13] X. Ke, S.A. Bernal, N. Ye, J.L. Provis, J. Yang, One-part geopolymers based on thermally treated red mud/NaOH blends, *J. Am. Ceram. Soc.* 98(1) (2015) 5-11.
- [14] N. Ye, J. Yang, S. Liang, Y. Hu, J. Hu, B. Xiao, Q. Huang, Synthesis and strength optimization of one-part geopolymer based on red mud, *Construction and Building Materials* 111 (2016) 317-325.
- [15] D. Ravikumar, N. Neithalath, An electrical impedance investigation into the chloride ion transport resistance of alkali silicate powder activated slag concretes, *Cement and Concrete Composites* 44 (2013) 58-68.
- [16] D. Rieger, T. Kovářik, J. Říha, R. Medlín, P. Novotný, P. Bělský, J. Kadlec, P. Holba, Effect of thermal treatment on reactivity and mechanical properties of alkali activated shale-slag binder, *Construction and Building Materials* 83 (2015) 26-33.
- [17] M.B. Karakoç, İ. Türkmen, M.M. Maraş, F. Kantarci, R. Demirboğa, M.U. Toprak, Mechanical properties and setting time of ferrochrome slag based geopolymer paste and mortar, *Construction and Building Materials* 72 (2014) 283-292.
- [18] C. Li, H. Sun, L. Li, A review: The comparison between alkali-activated slag (Si+ Ca) and metakaolin (Si+ Al) cements, *Cem. Concr. Res.* 40(9) (2010) 1341-1349.
- [19] I. Lecomte, M. Liégeois, A. Rulmont, R. Cloots, F. Maseri, Synthesis and characterization of new inorganic polymeric composites based on kaolin or white clay and on ground-granulated blast furnace slag, *Journal of materials research* 18(11) (2003) 2571-2579.
- [20] J. Xiang, L. Liu, Y. He, N. Zhang, X. Cui, Early mechanical properties and microstructural evolution of slag/metakaolin-based geopolymers exposed to karst water, *Cement and Concrete Composites* 99 (2019) 140-150.
- [21] P. Chindapasirt, T. Chareerat, S. Hatanaka, T. Cao, High-strength geopolymer using fine high-calcium fly ash, *J. Mater. Civ. Eng.* 23(3) (2011) 264-270.
- [22] H. Xu, W. Gong, L. Syltebo, K. Izzo, W. Lutze, I.L. Pegg, Effect of blast furnace slag grades on fly ash based geopolymer waste forms, *Fuel* 133 (2014) 332-340.
- [23] I. Ismail, S.A. Bernal, J.L. Provis, R. San Nicolas, S. Hamdan, J.S. van Deventer, Modification of phase evolution in alkali-activated blast furnace slag by the incorporation of fly ash, *Cement and Concrete Composites* 45 (2014) 125-135.
- [24] S. Kumar, R. Kumar, S. Mehrotra, Influence of granulated blast furnace slag on the reaction, structure and properties of fly ash based geopolymer, *Journal of materials science* 45(3) (2010) 607-615.
- [25] Y. Liu, W. Zhu, E.-H. Yang, Alkali-activated ground granulated blast-furnace slag incorporating incinerator fly ash as a potential

- binder, *Construction and Building Materials* 112 (2016) 1005-1012.
- [26] S. El-Gamal, F. Selim, Utilization of some industrial wastes for eco-friendly cement production, *Sustainable Materials and Technologies* 12 (2017) 9-17.
- [27] C.K. Yip, G. Lukey, J.S. Van Deventer, The coexistence of geopolymeric gel and calcium silicate hydrate at the early stage of alkaline activation, *Cem. Concr. Res.* 35(9) (2005) 1688-1697.
- [28] D. Nasr, A.H. Pakshir, H. Ghayour, The influence of curing conditions and alkaline activator concentration on elevated temperature behavior of alkali activated slag (AAS) mortars, *Construction and Building Materials* 190 (2018) 108-119.
- [29] M. Zawrah, R. Gado, R. Khattab, Optimization of slag content and properties improvement of metakaolin-slag geopolymer mixes, *The Open Materials Science Journal* 12(1) (2018).
- [30] U. Rattanasak, K. Pankhet, P. Chindaprasirt, Effect of chemical admixtures on properties of high-calcium fly ash geopolymer, *International Journal of Minerals, Metallurgy, and Materials* 18(3) (2011) 364.
- [31] F. Hashem, Sulfate attack on hardened Portland cement pastes with different porosities in presence of water-repelling admixtures, *Advances in cement research* 21(2) (2009) 75-82.
- [32] H.E. Elyamany, M. Abd Elmoaty, A.M. Elshaboury, Magnesium sulfate resistance of geopolymer mortar, *Construction and Building Materials* 184 (2018) 111-127.
- [33] J. Ye, W. Zhang, D. Shi, Effect of elevated temperature on the properties of geopolymer synthesized from calcined ore-dressing tailing of bauxite and ground-granulated blast furnace slag, *Construction and Building Materials* 69 (2014) 41-48.
- [34] M.B. Haha, G. Le Saout, F. Winnefeld, B. Lothenbach, Influence of activator type on hydration kinetics, hydrate assemblage and microstructural development of alkali activated blast-furnace slags, *Cem. Concr. Res.* 41(3) (2011) 301-310.
- [35] P. Nath, P.K. Sarker, Effect of GGBFS on setting, workability and early strength properties of fly ash geopolymer concrete cured in ambient condition, *Construction and Building Materials* 66 (2014) 163-171.
- [36] H.-y. Zhang, V. Kodur, L. Cao, S.-l. Qi, Fiber reinforced geopolymers for fire resistance applications, *Procedia engineering* 71 (2014) 153-158.
- [37] M. Zawrah, R. Gado, N. Feltn, S. Ducourtieux, L. Devoille, Recycling and utilization assessment of waste fired clay bricks (Grog) with granulated blast-furnace slag for geopolymer production, *Process Saf. Environ. Prot.* 103 (2016) 237-251.
- [38] S.A. Bernal, E.D. Rodríguez, R.M. de Gutiérrez, M. Gordillo, J.L. Provis, Mechanical and thermal characterisation of geopolymers based on silicate-activated metakaolin/slag blends, *Journal of materials science* 46(16) (2011) 5477-5486.
- [39] Z. Li, S. Zhang, Y. Zuo, W. Chen, G. Ye, Chemical deformation of metakaolin based geopolymer, *Cem. Concr. Res.* 120 (2019) 108-118.
- [40] S.A. Bernal, J.L. Provis, V. Rose, R.M. De Gutierrez, Evolution of binder structure in sodium silicate-activated slag-metakaolin blends, *Cement and Concrete Composites* 33(1) (2011) 46-54.
- [41] I.G. Lodeiro, D.E. Macphee, A. Palomo, A. Fernández-Jiménez, Effect of alkalis on fresh C-S-H gels. FTIR analysis, *Cem. Concr. Res.* 39(3) (2009) 147-153.